

The class II phosphoinositide 3-kinases PI3K-C2 α and PI3K-C2 β differentially regulate clathrin-dependent pinocytosis in human vascular endothelial cells

メタデータ	言語: eng 出版者: 公開日: 2019-04-25 キーワード (Ja): キーワード (En): 作成者: メールアドレス: 所属:
URL	https://doi.org/10.24517/00053883

This work is licensed under a Creative Commons
Attribution-NonCommercial-ShareAlike 3.0
International License.



1 **Class II phosphoinositide 3-kinases, PI3K-C2 α and PI3K-C2 β ,**
2 **differentially regulate clathrin-dependent pinocytosis in human**
3 **vascular endothelial cells**

4

5 Khin Thuzar Aung¹, Kazuaki Yoshioka¹, Sho Aki¹, Kazuhiro Ishimaru¹, Noriko

6 Takuwa^{1,2} and Yoh Takuwa^{1*}

7

8 1) Department of Physiology, Kanazawa University School of Medicine, Kanazawa,

9 Ishikawa 920-0934, Japan

10 2) Department of Health Science, Ishikawa Prefectural University, Kahoku,

11 Ishikawa 929-1210, Japan

12

13 *Corresponding author: Yoh Takuwa, M.D., Ph.D.

14 ytakuwa@med.kanazawa-u.ac.jp

15 TEL +81-76-265-2165, FAX +81-76-265-4223

16

17 **Author contributions**

18 K.T.A., K.Y., S.A., and Y.T. designed the study. K.T.A., K.Y., and S.A. performed

19 experiments. K.I. and N.T. helped experiments. K.T.A., K.Y., S.A., and Y.T. analyzed

20 the data. K.T.A., K.Y., and Y.T. wrote the manuscript. N.T. helped to draft the

21 manuscript. All authors approved the final version of the manuscript.

22

23

1 **Abstract**

2 Pinocytosis is an important fundamental cellular process to transport fluid and solutes.
3 Phosphoinositide 3-kinases (PI3Ks) regulate a diverse array of dynamic membrane events.
4 However, it is not well-understood which PI3K isoforms are involved in pinocytosis by
5 specific mechanisms. We found by siRNA-mediated knockdown that class II PI3K,
6 PI3K-C2 α and PI3K-C2 β , but not class I or III PI3K were required for pinocytosis, as
7 evaluated with FITC-dextran uptake, in endothelial cells. Pinocytosis was partially
8 dependent on both clathrin and dynamin, and both PI3K-C2 α and PI3K-C2 β were
9 required for clathrin-mediated, but not clathrin-non-mediated, FITC-dextran uptake at the
10 step up to its delivery to early endosomes. Both PI3K-C2 α and PI3K-C2 β were co-
11 localized with clathrin-coated pits and vesicles. However, PI3K-C2 β but not PI3K-C2 α
12 was highly co-localized with actin filament-associated clathrin-coated structures, and
13 required for actin filament formation at the clathrin-coated structures. These results
14 indicate that PI3K-C2 α and PI3K-C2 β play differential, indispensable roles in clathrin-
15 mediated pinocytosis.

16

17

18 **Keywords:** class II PI3K, PI3K-C2 α , PI3K-C2 β , pinocytosis, clathrin, endothelial cell

19

20

21

22

23

1 **Introduction**

2 Pinocytosis or fluid-phase endocytosis is one of the endocytic processes and engulfs
3 extracellular fluid into the endocytic vesicles [1]. The known processes for the endocytic
4 vesicle formation include clathrin-dependent, caveolin-dependent, and clathrin- and
5 caveolin-independent ones [2,3]. Among these, clathrin-dependent endocytosis is best
6 characterized. Clathrin-dependent endocytosis begins with the formation of invaginations
7 or pits at the plasma membrane and endocytic vesicles are formed by pinching-off at the
8 invagination neck by dynamin. In the processes, a complex protein machinery works
9 along with clathrins. The actin cytoskeletons are organized at clathrin-coated pits (actin
10 patches) and participate in growth of clathrin-coated pits. Pinocytosis takes place in
11 almost all types of cells. In particular, pinocytosis in blood capillary endothelial cells has
12 been recognized as an important portal of trans-endothelial transport of proteins, lipids
13 and lipoproteins, drugs, and cell-secreted exosomes and microparticles [4].

14 Endocytic processes are regulated by polyphosphoinositides (PPI) [5], small G
15 proteins including Rab [6], and other proteins [7]. PPIs are produced by phosphorylation
16 of the inositol ring by the actions of phosphoinositide kinases. Among these,
17 phosphoinositide 3-kinases (PI3K), which catalyze the phosphorylation of the D3
18 position within the inositol ring, play particularly important roles in membrane traffics
19 including endocytosis. PI3K comprise three classes: class I PI3Ks are activated mainly by
20 receptor tyrosine kinases and G protein-coupled receptors to exert cell proliferation,
21 migration and control of cell metabolism by generating PI(3,4)P₂ and PI(3,4,5)P₃ [8-10].
22 Class III PI3K, Vps34, stimulates the autophagic pathway by generating PI(3)P [11, 12].
23 In contrast to class I and class III PI3K, the roles of class II PI3K, which comprises PI3K-

1 C2 α , -C2 β and -C2 γ , were poorly understood. However, recent studies including ours
2 have shown that PI3K-C2 α is required for endocytosis of membrane proteins such as
3 vascular endothelial growth factor receptor and sphingosine-1-phosphate receptor while
4 PI3K-C2 β is involved in the regulation of autophagy [13-17]. The molecular and cellular
5 mechanisms of pinocytosis including clathrin-dependence or -independence and
6 requirement of PI3K are not fully understood.

7 Of three members of class II PI3K, PI3K-C2 α and PI3K-C2 β , are highly
8 homologous and widely expressed whereas PI3K-C2 γ shows less homology to PI3K-C2 α
9 and PI3K-C2 β and restricted expression in certain organs including liver and prostate [18,
10 19]. Therefore, in the present study we addressed whether and how class II PI3K-C2 α
11 and -C2 β are involved in pinocytosis in human vascular endothelial cells. We found that
12 PI3K-C2 α and -C2 β were both required for the clathrin-dependent, but not clathrin-
13 independent, pinocytosis. Interestingly, super-resolution microscopy revealed that not
14 only PI3K-C2 α but PI3K-C2 β were co-localized to clathrin-coated pits and vesicles, but
15 that only PI3K-C2 β was highly co-localized to actin filament (F-actin)-associated,
16 clathrin-coated pits and vesicles. These observations suggest that PI3K-C2 α and PI3K-
17 C2 β are involved in clathrin-mediated pinocytosis through the different mechanisms.

18
19
20

1 **Materials and Methods**

2 **Cell culture, reagents and transfection**

3 Human umbilical vein endothelial cells (HUVEC) (catalog no. C2517A; Lonza, Basel,
4 Switzerland) were plated on type-I collagen (Nitta Gelatin, Osaka, Japan)-coated dishes
5 and cultured in endothelial growth medium (EGM-2) with 2% fetal bovine serum (FBS)
6 and growth factors supplemented cocktails (catalog no. CC-3162; Lonza) at 37°C under
7 5% CO₂. Cells between passage 4 to 6 were used for experiments. Chemical inhibitors
8 used in this study were Pitstop-2 (catalog no. ab1206871; Abcam, Cambridge, UK),
9 wortmannin (WMN) (catalog no. 681675; Calbiochem, Darmstadt, Germany), GDC-
10 0941(Pictilisib) (catalog no. ab141352; Abcam) and 3-methyladenine (3-MA) (catalog no.
11 S-2767, Selleck Chemicals, Japan). Knockdown of endogenous PI3K isoforms and
12 clathrin heavy chain-1 (CHC) were performed with small interference RNA (siRNA)
13 transfection unless otherwise stated. siRNAs used in this study were synthesized using a
14 Silencer siRNA construction kit (catalog no. AM1620; Ambion, Austin, TX) according to
15 the manufacturer's protocol. The targeted sequences of siRNA were
16 5'-AAGGUUGGCACUUACAAGAAU-3' for human PI3K-C2 α (*PIK3C2A*),
17 5'- AAGCCGGAAGCUUCUGGGUUU-3' for human PI3K-C2 β (*PIK3C2B*),
18 5'- AAACUCAACACUGGCUAAUUA-3'for human Vps34 (*PIK3C3*),
19 5'-GGACAACUGUUUCAUAUAG-3' for human PI3K p110 α (*PIK3CA*),
20 5'-AAUCCAAUUCGAAGACCAAUU-3' for human CHC-1 (CLTC). Intersectin1
21 (ITSN1) siRNAs was purchased from Invitrogen (catalog no.10620318) and the targeted
22 sequence was 5'-GGAAUCGAAGGCAAGAACUACUAAA-3'. The scrambled siRNA
23 sequence was 5'- AAUUCUCCGAACGUGUCACGU-3'. Cells were transiently

1 transfected with specific siRNA and Lipofectamine 2000 (catalog no.11668-019;
2 Invitrogen-Thermo Fisher Scientific, Waltham, MA, USA) or Lipofectamine RNAiMAX
3 (catalog no.13778075; Invitrogen) in Opti-MEM (catalog no.31985070, Invitrogen)
4 according to manufacturer's instruction for 48-72 hr before the experiments. The single
5 knockdown was conducted by transfecting cells with 50 nM of siRNA whereas the
6 double knockdown was conducted by the transfection with the two specific siRNAs at 25
7 nM each. The transfection efficiency of siRNA, as evaluated with fluorescent dye
8 (FAM)-labelled negative control siRNA No.1 (5'-AGUACUGCUUACGAUACGGTT-
9 3') (catalog no. AM4620, Ambion), was 94 % in HUVEC. The efficiency of siRNA
10 mediated knockdown was confirmed by Western blotting using specific antibodies.

11 The enhanced green fluorescent protein (GFP)-tagged PI3K-C2 α (GFP-C2 α)
12 expression vector was described as previously [13]. PI3K-C2 β complimentary DNA
13 (cDNA) was obtained from K. Kitatani (Setsunan University, Osaka) [20]. For the
14 expression vector for mCherry-tagged PI3K-C2 α (mCherry-C2 α) and GFP- or mCherry-
15 tagged PI3K-C2 β (GFP-C2 β , mCherry-C2 β), human *PIK3C2A* and *PIK3C2B* cDNA
16 fragments were amplified by PCR using PrimeSTAR HS DNA Polymerase (catalog no.
17 R010A; Takara-Bio Company, Shiga, Japan) according to the manufacturer's protocol.
18 Sub-cloning of the PCR products into pmCherry-C1 (catalog no. 632524; Clontech-
19 Takara Bio Inc, Shiga, Japan) and pAcGFP1-N vectors (catalog no. 632501; Clontech)
20 was performed using In-Fusion HD Cloning Kit (catalog no. Z9633N; Clontech).
21 Monomeric red fluorescent protein (mRFP)-tagged wild-type dynamin-2 (WT-dynamin2)
22 and dominant negative K44A mutant of dynamin-2 (K44A-dynamin2) were kindly
23 provided by Dr. Pietro De Camilli, Yale University School of Medicine (De Camilli,

1 2009). mEmerald-Lifeact-7 were gifts from Michael Davidson (Addgene plasmid #54148
2 and #56249, respectively). mRFP-clathrin light chain (CLC) was a gift from Ari Helenius
3 (Addgene plasmid #14435). GFP-intersectin1 short-isoform (ITSN1s) was a gift from
4 Peter McPherson (Addgene plasmid #47394). All plasmids were purified using
5 Endotoxin-Free Plasmid Maxi Kit (catalog no.12362; Qiagen, Germany). Cells were
6 transfected with expression plasmids using Nucleofactor-I electroporation device
7 (Program A-034, Lonza) with Amaxa Nucleofector kit (catalog no. VPB-1002; Lonza).

8 For visualization of early endosomes in live cells, cells were transiently
9 transduced with the RFP-Rab5 expression vector (CellLight™ Early Endosomes-RFP)
10 according to manufacturer's instructions (catalog no. C10587, Invitrogen). In brief, cells
11 were plated at a density of 1×10^4 cells in 35-mm glass bottomed dishes (catalog no. P
12 35G-0-14-C; MatTek Co., Ashland, MA, USA) 1 day before transduction. Cells were
13 incubated with EGM-2 medium containing 5 μ l of BacMam reagent at 37°C under 5 %
14 CO₂ for 12-16 hr and the medium was replaced with fresh EGM-2. The experiment was
15 carried out after 4 hr of recovery.

16

17 **Fluorescent labelled-dextran uptake assay**

18 HUVECs that had been grown in EGM-2 overnight after plating were incubated with 0.2
19 or 0.5 mg/ml concentration of fluorescein isothiocyanate (FITC)-dextran (70-kD M.W.,
20 catalog no.# 60842-46-8; Sigma, St. Louis, MO) or AlexaFluor647-dextran (10-kDa
21 M.W., catalog no. D 22914; Molecular Probes-Thermo Fisher Scientific) at 37 °C for
22 indicated time periods. After washing with Ca²⁺- and Mg²⁺-free Dulbecco's phosphate
23 buffered saline (PBS), the cells were fixed with 4% paraformaldehyde (PFA, Wako) and

1 stained with 4',6-diamidino-2-phenylindole (DAPI) (catalog no. D1306; Molecular
2 probes, Eugene, OR). For pulse-chase analysis of dextran, cells were incubated for 1 hr
3 with 0.5 mg/mL FITC-dextran at 37 °C in growth medium, washed twice with growth
4 medium, and were placed in a CO₂ incubator. At the indicated time points, cells were
5 fixed with 4% PFA for 10 min and stained with DAPI. Fluorescence images were
6 captured with confocal microscopy as described below. Image acquisition and processing
7 were performed with iQ software (Andor, UK). FITC-dextran uptake was quantified by
8 using 'Analyze Particles' feature in Fiji (Image J) software.

9

10 **Western blotting**

11 Total cell lysates were prepared by scraping PBS-washed cells in 2x Laemmli SDS-
12 PAGE sample buffer on ice 48 hr after siRNA transfection. The samples were separated
13 on 8% SDS-PAGE, followed by electrotransfer onto PVDF membranes (catalog no.
14 IPV00010; Immobilon-P, Millipore-Merck, Nottingham, UK) using Trans-Blot Turbo
15 blotting system (Bio-Rad, Richmond, CA). The membranes were blocked in 5% bovine
16 serum albumin (BSA) and 0.1% Tween-80 in Tris-buffered saline (TBS) for 1 hr and
17 incubated with specific antibodies at 4 °C overnight. The antibodies used are PI3K-C2 α
18 (1:1000) (catalog no.12402; Cell Signaling Technology (CST), Danvers, MA, USA.),
19 PI3K-C2 β (1:1000) (catalog no. 611342; BD transduction laboratories, USA), p110 α
20 (1:1000) (catalog no. 4249; CST), Vps34 (1:1000) (catalog no. 4263, CST), Clathrin
21 heavy chain (1:1000) (catalog no. ab21679, Abcam) and GAPDH (1:1000) (catalog no.
22 016-25523, Wako). The membranes were incubated with alkaline phosphatase-
23 conjugated secondary antibodies anti-rabbit IgG antibody (1:1000) (catalog no. 7054,

1 CST), anti-mouse IgG antibody (1:1000) (catalog no. 7056, CST) for 1 hr at room
2 temperature and protein bands were visualized by color reaction using nitro blue
3 tetrazolium (NBT,WAKO)/ 5-bromo-4-choloro-3'-indolylphosphate p-toluidine (BCIP,
4 WAKO) system. Protein band intensities were determined using Image Studio lite
5 software (LI-COR).

6

7 **Immunostaining**

8 HUVECs were plated onto type I collagen-coated glass bottom dishes and allowed to
9 adhere to dishes in EGM-2 overnight. The cells were rinsed with PBS once and fixed
10 with 4% PFA in 0.1M phosphate buffer (pH 7.4) for 10 min at room temperature. Then
11 permeabilization was done with 0.3% TritonX-100 in PBS for 15 min or 90% chilled
12 methanol for 5min. After blocking in 5% normal goat serum (NGS, Wako) / 0.3%
13 TritonX-100 in PBS, the cells were incubated with indicated primary antibodies
14 overnight at 4 °C. The antibodies used are PI3K-C2 β (1:500) (catalog no. 611342; BD
15 transduction laboratories, USA), clathrin heavy chain (1:400) (catalog no. ab21679,
16 Abcam), clathrin heavy chain (1:400) (catalog no.MA1-065, ThermoFisher Scientific),
17 EEA1 (1:200) (catalog no. 610456, BD), EEA1 (1:200) (catalog no. PA1-063A,
18 ThermoFisher Scientific), Rab7 (1:100) (catalog no. 9367, CST), LAMP1 (1:200)
19 (catalog no. 328601, BioLegend), LC3B (1:400) (catalog no. 3868, CST) and ITSN1
20 (1:400) (catalog no. ab118262, Abcam). After washing with 0.1% TritonX-100 in PBS,
21 the cells were incubated with appropriate Alexa Flour-conjugated secondary antibodies
22 (Molecular probes) for 1 hr at room temperature. For F-actin staining, HUVEC were
23 washed with prewarmed PBS for 2 times, fixed with 4% PFA and permeabilized in 0.2%

1 Triton X-100 for 5 min. After that cells were stained with iFluor488-conjugated
2 Phalloidin (catalog no. 0549, Cayman Chemical, Ann Arbor, USA) or AlexaFlour594-
3 conjugated phalloidin (catalog no. 12381, Molecular Probes) according to manufacturer's
4 instruction. The cells were counterstained with DAPI for 30 min.

5

6 **Confocal microscopy and super-resolution radial fluctuation (SRRF)-Stream** 7 **imaging**

8 Results from Figs.1, 2 and 5 were carried out on a custom confocal microscope based on
9 an inverted IX70 microscope (Olympus) equipped with an UPLSAPO 60X/NA1.35-oil
10 Objective, a confocal disk-scanning unit (CSU10, Yokogawa, Tokyo) and EMCCD
11 camera (iXon DV887, Andor Technologies) as described previously [13]. The acquisition
12 and process were controlled by iQ software (Andor Technologies). All other observations
13 and live-cell imaging were carried out on an inverted Nikon Eclipse Ti2 confocal
14 microscope (Nikon Instruments) with the Perfect Focus System, attached to an Andor
15 Dragonfly spinning-disk unit, Andor EMCCD camera (iXon DU888, Andor
16 Technologies) and a laser unit (Coherent). An oil-immersion objective (PlanApo 60X,
17 NA 1.4, Nikon) was used for all experiments. Excitation for BFP/DAPI,
18 GFP/mEmerald/Alexa488, mRFP/mCherry/Alexa568 and Alexa647 chromophores was
19 provided by 405, 488, 561 and 637 nm laser, respectively. Super-resolution imaging of
20 fixed cells was performed using an Andor Dragonfly confocal microscope in SRRF-
21 Stream mode. Live-cell imaging of multicolor-labelled cells plated on collagen-coated
22 glass-bottom dishes was performed in EGM-2 containing 2% FBS at 37 °C with 5% CO₂
23 in a humidified incubator (Tokai-Hit) using the confocal microscope in SRRF-Stream

1 mode as described above. Live-cells were maintained in the imaging incubator for up to
2 30 min. Time-lapse images were taken at every 10-s interval using Andor Fusion
3 software, and movies were prepared at a frequency of 20 frames/s using Imaris software
4 (Bitplane, Oxford Instruments). To minimize sample drift in the z-direction over time a
5 motorized-Piezo stage controlled by a near infrared-light adjusted Perfect Focus System
6 (Nikon Instruments) was applied. Images were quantified using Fiji (ImageJ) software,
7 and area and shape characteristics were measured using the Analyze Particles in Fiji
8 (ImageJ).

9

10 **Statistical analysis**

11 Statistical analysis was performed with Prism 7 software (GraphPad Software). *N* of 3 or
12 more than that in sample numbers was acquired for quantitative WB analysis and image
13 analysis. Data were presented as mean \pm standard errors of mean (SEM), or median and
14 interquartile range with error bars denoting minimal and maximal values. For comparison
15 between multiple groups, one or two ways ANOVA followed by Bonferroni post hoc test
16 was used unless stated otherwise. *p* value < 0.05 was considered to be statistically
17 significant.

18

19

20

21

22

23

1 **Results**

2 **Class II PI3K-C2 α and PI3K-C2 β are necessary for pinocytosis**

3 We studied the roles of PI3K-C2 α and -C2 β in the pinocytic activity at steady-state in
4 HUVEC, a best-characterized human primary vascular endothelial cell. We evaluated
5 pinocytic activity by determining time-dependent uptake of a fluid-phase marker FITC-
6 dextran into cells. FITC-dextran uptake was increased in a time-dependent manner (Fig.
7 1a and b). To study roles of PI3K isoforms in pinocytosis, we investigated the effects of
8 siRNA-mediated knockdown of individual PI3K isoforms on FITC-dextran uptake. The
9 siRNAs specific to class II PI3K-C2 α and -C2 β , class I p110 α , and class III Vps34
10 effectively and specifically inhibited the protein expression of respective PI3K isoforms
11 (Fig. 1c). Knockdown of PI3K-C2 α or PI3K-C2 β partially but significantly (53 and 70%,
12 respectively) decreased FITC-dextran uptake, compared with scrambled siRNA
13 transfection (Fig. 1d and e). In contrast, knockdown of either p110 α or Vps34 did not
14 inhibit FITC-dextran uptake. We also studied the effects of pharmacological PI3K
15 inhibitors on pinocytic activity. Treatment of cells with a higher dose (1 μ M) of the pan-
16 PI3K inhibitor WMN caused a reduction in FITC-dextran uptake compared with vehicle-
17 treated cells. However, a lower dose (30 nM) of WMN, the class I PI3K inhibitor GDC-
18 0941, or the Vps34-specific inhibitor 3-MA failed to inhibit FITC-dextran uptake (Fig.
19 1f). These data suggest that class II PI3K-C2 α and PI3K-C2 β , but not class I p110 α or
20 class III Vps34, are involved in fluid-phase pinocytosis in HUVECs.

21

22 **Pinocytosis in HUVECs is partially dependent on clathrin and dynamin**

1 We examined whether pinocytosis at steady-state in HUVECs required clathrin and
2 dynamin or not. The clathrin inhibitor, Pitstop-2, inhibited FITC-dextran uptake by
3 approximately 69 % (Fig. 2a). Similarly, siRNA-mediated knockdown of clathrin heavy
4 chain (CHC) inhibited FITC-dextran uptake by approximately 55 % (Fig. 2b).
5 Furthermore, the expression of the dominant negative mutant (K44A) of dynamin-2 (dn-
6 Dyn2) inhibited the FITC-dextran uptake by approximately 53 % (Fig. 2c). These
7 observations indicate that pinocytosis is at least partially mediated by clathrin- and
8 dynamin-dependent processes in HUVECs. Interestingly, the extents of inhibition by the
9 inhibitor, the knockdown and the mutant protein were roughly similar to those induced by
10 knockdown of PI3K-C2 α and PI3K-C2 β (Fig. 1e).

11

12 **Partially overlapping subcellular localization of PI3K-C2 α and PI3K-C2 β**

13 We studied the subcellular localization of PI3K-C2 α and PI3K-C2 β in HUVECs that
14 expressed GFP-C2 α and mCherry-C2 β , using super-resolution microscopy. GFP-C2 α
15 was distributed as fine puncta widely throughout the cells whereas mCherry-C2 β was
16 enriched mainly in the perinuclear region as coarse puncta, the peripheral regions
17 surrounding podosomes as coarse and fine puncta, and the plasma membrane (Fig. 3a). A
18 substantial portion of mCherry-C2 β in the cell periphery was closely associated with F-
19 actin structures (membrane ruffles and small F-actin assembly (actin patches)) (Fig. 3b
20 right). In contrast, GFP-C2 α was barely associated with the F-actin structures (Fig. 3b
21 left). The punctate fluorescence of GFP-C2 α overlapped strikingly with clathrin-coated
22 pits and vesicles. A part of GFP-C2 α fluorescence was colocalized with EEA1-positive
23 (EEA1⁺) early endosomes (EE), and to much lesser extents with Rab7⁺ late endosomes

1 (LE), LAMP1⁺ lysosomes (LY), and LC3B⁺ autophagosomes (AP) (Fig. 3c). We and
2 others previously demonstrated the co-localization of PI3K-C2 α with clathrin-coated
3 structures and early endosomes, using anti-PI3K-C2 α immunostaining [13, 21-23]. In
4 contrast, PI3K-C2 β signals were less frequently colocalized with clathrin-coated pits and
5 vesicles compared with GFP-C2 α , and slightly colocalized with EE, LE and LY.
6 However, perinuclear PI3K-C2 β was highly colocalized with LC3B⁺-AP (Fig. 3d). Thus,
7 GFP-C2 α and mCherry-C2 β show the significantly different subcellular localization,
8 suggesting that PI3K-C2 α and -C2 β may differentially control pinocytic processes. We
9 also determined the subcellular localization of endogenous PI3K-C2 β using anti-PI3K-
10 C2 β immunostaining. Endogenous PI3K-C2 β was partially colocalized with F-actin
11 structures, clathrin-coated structures and LC3B⁺ AP, and less frequently with EEA1⁺ EEs
12 (Fig. 4), which was similar to the results obtained with mCherry-C2 β expression (Fig. 3d).

13

14 **PI3K-C2 α and -C2 β are required for clathrin-mediated pinocytosis**

15 To gain further insight into the regulation of pinocytosis by PI3K-C2 α and PI3K-C2 β , we
16 examined the effects of double knockdown of PI3K-C2 α and PI3K-C2 β mRNAs on
17 pinocytosis. The double knockdown of PI3K-C2 α and -C2 β gave the similar extents of
18 suppression of the PI3K-C2 α and -C2 β protein expression and the FITC-dextran uptake
19 compared with the single knockdown of either PI3K-C2 α or PI3K-C2 β (Fig. 5a). We next
20 examined which of clathrin-dependent and -independent endocytic mechanisms in
21 pinocytosis requires PI3K-C2 α and -C2 β . Knockdown of CHC inhibited FITC-dextran
22 uptake. Double knockdown of clathrin-heavy chain (CHC) and either of PI3K-C2 α and
23 PI3K-C2 β did not result in further inhibition of FITC-dextran uptake compared with

1 inhibition by CHC single knockdown (Fig. 5b). These findings suggest that both PI3K-
2 C2 α and -C2 β are required for clathrin-dependent, but not clathrin-independent,
3 pinocytosis. Since single knockdown of either PI3K-C2 α or -C2 β results in complete
4 inhibition of the clathrin-mediated pinocytosis, the two isoforms play non-redundant,
5 distinct roles in clathrin-mediated pinocytosis.

6 Live-cell super-resolution imaging of the cells transfected with either GFP-C2 α or
7 GFP-C2 β and mRFP-clathrin light chain (CLC) showed that GFP-C2 α formed dynamic
8 puncta that were mostly colocalized with mRFP-CLC (Fig. 5c and Supplementary movie
9 1). GFP-C2 β was also colocalized with mRFP-CLC puncta, but the colocalization was
10 less abundant compared with the case of PI3K-C2 α (Fig. 5d and Supplementary movie 2).
11 The serial magnified images showed that PI3K-C2 α and -C2 β were recruited to mRFP-
12 CLC puncta and then the clathrin was disassembled, followed by the dissociation of GFP-
13 C2 α and GFP-C2 β (Fig. 5c and d (lower panels), and e). The fluid-phase marker
14 Alexa647-dextran was found in vesicles double-positive for mRFP-CLC and either GFP-
15 C2 α or -C2 β (Fig. 5f), provided morphological evidence that the dextran was
16 pinocytosed at least in part into PI3K-C2 α and -C2 β -associated clathrin-coated vesicles.

17 Since clathrin-coated pinocytic vesicles are transported to early endosomes, we
18 examined the effects of knockdown of PI3K-C2 α and -C2 β on FITC-dextran
19 accumulation in EEs in the cells expressing the EE marker mRFP-Rab5. Knockdown of
20 either PI3K-C2 α or PI3K-C2 β reduced the numbers of FITC-dextran puncta in Rab5⁺ EE
21 after 60 min uptake of FITC-dextran without any change in the number of Rab5⁺ EE (Fig.
22 5g). We determined time course of degradation of internalized FITC-dextran using pulse-
23 chase experiments. After 60 min uptake of FITC-dextran, the cells were washed and

1 monitored for FITC-dextran remaining in cells for up to 8 hr. The number of FITC-
2 dextran within either PI3K-C2 α - or PI3K-C2 β -depleted cells gradually decreased with
3 the similar time course, compared with scrambled siRNA-transfected cells (Fig. 5h),
4 suggesting that degradation of uptaken FITC-dextran was not altered by knockdown of
5 PI3K-C2 α or -C2 β . The findings collectively suggest that both PI3K-C2 α and PI3K-C2 β
6 are involved in the early step(s) of clathrin-mediated pinocytic pathway, namely the
7 process up to FITC-dextran delivery to the Rab5⁺-EE.

8

9 **PI3K-C2 β is required for the formation of pinocytic vesicle-associated actin**

10 **filaments**

11 Since we found the colocalization of class II PI3Ks, particularly PI3K-C2 β , with F-actin
12 in the present study (Fig. 3) and actin polymerization at clathrin-coated pits and vesicles
13 is reportedly required for pit maturation and vesicle formation [24-26], we studied roles
14 of PI3K-C2 α and -C2 β in the F-actin formation at clathrin-coated pits, using super-
15 resolution microscopy. The cells that had been transfected with mRFP-CLC and GFP-
16 tagged F-actin-binding peptide, mEmerald-Lifeact, were subjected to uptake of
17 Alexa647-dextran. Like the case of FITC-dextran uptake, knockdown of PI3K-C2 α or -
18 C2 β substantially inhibited Alexa647-dextran uptake (Fig. 6a-d). Many of dextran-
19 containing pinocytic vesicles were associated with F-actin (actin patches) (Fig. 6a). A
20 substantial portion of clathrin-coated pits and vesicles was associated with actin patches.
21 Knockdown of PI3K-C2 β greatly reduced the formation of clathrin-associated actin
22 patches (Fig. 6a-c and e). Moreover, knockdown of PI3K-C2 β but not PI3K-C2 α reduced
23 the colocalization of actin patches and dextran (Fig. 6a-c and f). Consistent with this,

1 dextran-positive pinocytic vesicles that were associated with F-actin (white arrowheads in
2 Fig. 6a and c) were decreased in PI3K-C2 β -depleted cells. Instead, pinocytic vesicles that
3 were not associated with F-actin were relatively increased in PI3K-C2 β -depleted cells
4 (yellow arrows). These observations suggest that PI3K-C2 β facilitates actin patch
5 formation at clathrin-coated structures to promote clathrin-mediated pinocytosis.

6

7 **Overexpression of PI3K-C2 β but not PI3K-C2 α enhances the uptake of dextran**

8 We studied whether overexpression of mCherry-PI3K-C2 α and -C2 β affected pinocytosis.
9 ITSN1, which was originally found to be localized in clathrin coated pits [27], has been
10 very recently identified as a multifunctional scaffold protein that is required for actin
11 patch formation [28]. The short form of ITSN1 (ITSN1s) was also previously shown to
12 bind PI3K-C2 β [29]. Therefore, we compared the effects of PI3K-C2 α and -C2 β
13 overexpression with and without expression of GFP-tagged ITSN1s (GFP-ITSN1s).
14 mCherry-C2 β expression increased dextran uptake only when GFP-ITSN1s was co-
15 expressed (Fig. 7a and b). Interestingly, the expression of GFP-ITSN1s recruited
16 mCherry-C2 β from the cytoplasmic pool to GFP-ITSN1s-localized structures (Fig. 7a).
17 In contrast, PI3K-C2 α overexpression did not increase dextran uptake or induce PI3K-
18 C2 α recruitment to dot-like structures with or without ITSN1s overexpression (Fig. 7c
19 and d). These observations suggested that mCherry-C2 β overexpression stimulated
20 pinocytosis through the mechanisms involving GFP-ITSN1s-mediated recruitment of
21 mCherry-C2 β .

22

1 **Endogenous ITSN1 is required for the formation of actin patches and recruitment**
2 **of PI3K-C2 β to the clathrin-coated structures.**

3 We determined the impact of ITSN1 knockdown on F-actin structures and translocation
4 of endogenous PI3K-C2 β . In control cells, ITSN1 showed a punctate distribution pattern
5 with anti-ITSN1 staining, and was partially colocalized with actin patches and clathrin-
6 coated structures (Fig. 8a). ITSN1 knockdown effectively reduced ITSN1 expression
7 compared with control cells. ITSN1 knockdown severely impaired the formation of F-
8 actin structures including actin patches and stress fibers (Fig. 8a left). In contrast, ITSN1
9 knockdown did not affect the number of clathrin-coated structures (Fig. 8a right).

10 Interestingly, ITSN1-knockdown dramatically reduced the localization of PI3K-C2 β at
11 actin patches (Fig. 8b left) and clathrin-coated structures (Fig. 8b right). These data are
12 consistent with the notion that endogenous ITSN1 is required for the formation of
13 clathrin-associated actin patches and PI3K-C2 β localization at actin filament-associated
14 clathrin-coated structures.

15

1 **Discussion**

2 PI3Ks are recognized as crucial regulators for various membrane traffic events, which
3 include phagocytosis, macropinocytosis and autophagy through the PI3K class-specific
4 multiple mechanisms [11, 30-36]. The present study demonstrated that, among three
5 different PI3K classes, pinocytosis or fluid-phase endocytosis requires class II PI3K
6 PI3K-C2 α and PI3K-C2 β , but not class I p110 α or class III Vps34. Mechanistically, both
7 of these two class II PI3K isoforms are required for clathrin-mediated, but not clathrin-
8 non-mediated, pinocytosis very likely through the differential mechanisms.

9 Previous studies including ours [13, 14, 21-23] showed that PI3K-C2 α closely associates
10 with clathrin-coated pits and vesicles through the direct interaction via its N-terminal
11 clathrin-binding domain and that knockdown of PI3K-C2 α inhibited internalization of
12 cell surface molecules. In contrast, little was understood about a role of PI3K-C2 β in the
13 regulation of endocytosis. Pinocytosis in HUVECs comprised clathrin-mediated and -
14 non-mediated one, as assayed by dextran uptake. Our data of the double knockdown
15 experiments showed that both PI3K-C2 α and PI3K-C2 β participate in clathrin-mediated,
16 but not -non-mediated, pinocytosis. Interestingly, because knockdown of either one of
17 PI3K-C2 α and PI3K-C2 β induced the similar extents of inhibition of pinocytosis to
18 double knockdown of PI3K-C2 α and PI3K-C2 β , it is suggested that PI3K-C2 α and PI3K-
19 C2 β play distinct, non-redundant roles in clathrin-mediated pinocytosis.

20 A previous study [37] showed that mitotic spindle assembly required PI3K-C2 α
21 protein but not its kinase activity, suggesting a scaffold role of PI3K-C2 α in mitotic
22 spindle assembly. PI3K-C2 α is clearly less sensitive to pan-PI3K inhibitors WMN and
23 LY294002, and higher concentrations of both inhibitors are required for effective

1 inhibition of PI3K-C2 α compared with the other PI3K members [38, 39]. PI3K-C2 β is
2 more sensitive to the PI3K inhibitors compared with PI3K-C2 α , but is a little less
3 sensitive to the inhibitors compared with class I and III PI3Ks. In the present study, only
4 the higher concentration of WMN but not its lower concentration inhibited pinocytosis.
5 Based on previous reports [38, 39], the lower concentration of WMN is expected to
6 effectively inhibit class I and III PI3K but not PI3K-C2 α . It is difficult to conclude
7 whether PI3K-C2 β was effectively inhibited or not by the lower dose of WMN. Therefore,
8 these results could imply that the kinase activity of at least either one of PI3K-C2 α and
9 PI3K-C2 β is required for pinocytosis. In the case when one of PI3K-C2 α and PI3K-C2 β
10 acts via a kinase-independent mechanism, it could include a scaffold role [37, 40].
11 Further investigations are necessary to explore the possibility that PI3K-C2 α and PI3K-
12 C2 β regulate pinocytosis via kinase-independent mechanisms.

13 In this study, super-resolution microscopic imaging revealed the three novel
14 findings about the subcellular distribution and functions of class II PI3K in clathrin-
15 coated pits and vesicles: first, PI3K-C2 β as well as PI3K-C2 α were co-localized with
16 dextran-containing, clathrin-coated endocytic vesicles (Fig. 5f). PI3K-C2 β and PI3K-C2 α
17 exhibited the similar behaviors in the assembly and disassembly with clathrin-coated pits
18 and/or vesicles (Fig. 5 c-e). Second, the detailed microscopic analyses revealed
19 differences in their localization at clathrin-coated pits and/or vesicles: PI3K-C2 β showed
20 stronger colocalization with F-actin compared with PI3K-C2 α (Fig. 3) and was required
21 for the actin organization at dextran-containing, clathrin-coated structures (Fig. 6 c, e and
22 f). Third, PI3K-C2 β overexpression resulted in the different effects on dextran uptake and
23 the interaction with ITSN1 compared with PI3K-C2 α : the overexpression of PI3K-C2 β

1 but not PI3K-C2 α stimulated pinocytosis with the changes of PI3K-C2 β distribution in
2 the presence of overexpressed ITSN1.

3 The present study and previous studies suggest that PI3K-C2 α and PI3K-C2 β are
4 recruited to clathrin-coated pits and vesicles through the different mechanisms. It is
5 recognized that PI3K-C2 α is localized to clathrin-coated structures through its N-terminal
6 clathrin-binding domain and C-terminal PX-C2 module [22, 41]. The C-terminal PX-C2
7 module contributes to PI3K-C2 α recruitment to the clathrin-coated structures through the
8 binding to PI(4,5)P₂ on the membrane. The binding of PI3K-C2 α to the clathrin-coated
9 membrane relieves the intramolecular autoinhibition and enhances its enzymatic activity,
10 resulting in PI(3,4)P₂ accumulation [41]. Accumulation of PI(3,4)P₂ recruits the
11 PI(3,4)P₂-binding endocytic effector proteins including SNX9 at the clathrin-coated pits
12 to promote endocytosis. In contrast, PI3K-C2 β , which lacks the typical clathrin-binding
13 domain, likely requires a different mechanism for its recruitment to clathrin-coated
14 structures. A complex protein machinery which acts in the endocytic site includes ITSN1,
15 a multifunctional scaffold protein [28]. Importantly, ITSN1 was previously identified as a
16 binding partner of PI3K-C2 β through the interaction between its SH3 domain and
17 proline-rich region of PI3K-C2 β [29]. Consistent with this, our study showed that
18 ITSN1s overexpression changed the subcellular distribution of PI3K-C2 β , resulting in the
19 PI3K-C2 β distribution as many dots. Vice versa, knockdown of ITSN1 resulted in
20 decreased translocation of PI3K-C2 β into clathrin-coated structures. In contrast, PI3K-
21 C2 α does not possess such proline-rich region. Therefore, ITSN1s likely does not serve
22 as a binding partner for PI3K-C2 α . In fact, ITSN1s overexpression did not affect the
23 subcellular distribution of PI3K-C2 α in the present study. A recent study [28] showed

1 that in the endocytic site, ITSN1 also recruits the F-BAR domain-containing protein
2 FCHSD2, which stimulates actin polymerization via the activation of WASP family
3 proteins, resulting in the formation of actin patches around the clathrin-coated pits. Actin
4 cytoskeleton is involved in multiple steps of clathrin-coated vesicle formation, i.e.
5 nucleation for plasma membrane invagination, progression to form mature clathrin-
6 coated pits and scission to expel vesicles into the cytoplasm, thus facilitating endocytosis
7 [42-44]. The recruitment of the F-BAR protein FCHSD2 to the clathrin-coated pits and
8 vesicles is a key event for clathrin-coated vesicle formation, and relies on the interaction
9 of FCHSD2 with ITSN1 and the FCHSD2 binding to PI(3,4)P₂ on the membrane.
10 Therefore, PI3K-C2β may contribute to actin polymerization in the endocytic site through
11 generating PI(3,4)P₂ and recruiting FCHSD2. PI3K-C2α and PI3K-C2β are both large
12 multi-domain proteins and have the complex interactions with multiple proteins in the
13 clathrin-coated pits and vesicles. Therefore, although both PI3K mainly generate the
14 same lipid product PI(3,4)P₂, the functional roles that PI3K-C2α and PI3K-C2β play in
15 clathrin-coated vesicle formation are different.

16 In conclusion, our study indicates that PI3K-C2β as well as PI3K-C2α are
17 required for fluid-phase endocytosis. Our data collectively suggest that both PI3K-C2α
18 and PI3K-C2β participate in the clathrin-coated vesicle formation but through the
19 different mechanisms. PI3K-C2β promotes clathrin-coated vesicle formation very likely
20 through stimulating F-actin formation in the endocytic site. Thus, our study emphasizes
21 the involvement of two isoforms of class II PI3K in clathrin-mediated endocytosis.

22

1 **Acknowledgements**

2 We thank Ms. Chiemi Hirose for secretarial assistance, and also thank the members of
3 Department of Physiology for their support and assistance.

4

5

6 **Compliance with Ethical Standards**

7 **Sources of Funding:** This study was supported by grants from the Japan International
8 Cooperation Agency (JICA, J-14-10306 to KTA), the Ministry of Education, Culture,
9 Sports, Science and Technology (MEXT) of Japan (25116711 to Y.T.), and the Japan
10 Society for the Promotion of Science (17K08532 to K.Y., 16K18988 to S.A., 16K15409
11 to K.I., 17K08542 to N.T., 15H04673 to Y.T.). The funders had no role in study design,
12 data collection and analysis, decision to publish, or preparation of the manuscript.

13 **Conflict of Interest:** The authors declare that they have no conflict of interest.

14 **Ethical approval:** This article does not contain any studies with human participants or
15 animals performed by any of the authors.

16

17

18

19

20

21

22

23

1 **References**

- 2 1. Conner SD, Schmid SL (2003) Regulated portals of entry into the cell. *Nature*
3 422:37-44. doi:10.1038/nature01451
- 4 2. Doherty GJ, McMahon HT (2009). Mechanisms of endocytosis. *Annu Rev*
5 *Biochem* 78:857-902. doi:10.1146/annurev.biochem.78.081307.110540.
- 6 3. Kaksonen M, Roux A (2018) Mechanisms of clathrin-mediated endocytosis. *Nat*
7 *Rev Mol Cell Biol*. 19: 313-326. doi: 10.1038/nrm.2017.132.
- 8 4. Simionescu M, Gafencu A, Antohe F (2002) Transcytosis of plasma
9 macromolecules in endothelial cells: a cell biological survey. *Microsc Res Tech* 57: 269-
10 288. doi:10.1002/jemt.100865.
- 11 5. Bohdanowicz M, Grinstein S (2013) Role of phospholipids in endocytosis,
12 phagocytosis, and macropinocytosis. *Physiol Rev* 93:69–106.
13 doi:10.1152/physrev.00002.2012
- 14 6. Hutagalung AH, Novick PJ (2011) Role of Rab GTPases in membrane traffic and
15 cell physiology. *Physiol Rev* 91:119–149. doi:10.1152/physrev.00059.2009
- 16 7. Merrifield CJ (2004) Seeing is believing: Imaging actin dynamics at single sites
17 of endocytosis. *Trends Cell Biol* 14:352–358. doi:10.1016/j.tcb.2004.05.008
- 18 8. Hawkins PT, Anderson KE, Davidson K, Stephens LR (2006) Signalling through
19 class I PI3Ks in mammalian cells. *Biochem Soc Trans* 34:647–662.
20 doi:10.1042/BST0340647
- 21 9. Vanhaesebroeck B, Guillermet-Guibert J, Graupera M, Bilanges B (2010) The
22 emerging mechanisms of isoform-specific PI3K signalling. *Nat Rev Mol Cell Biol*
23 11:329–341. doi:10.1038/nrm2882

- 1 10. Jean S, Kiger AA (2014) Classes of phosphoinositide 3-kinases at a glance. *J Cell*
2 *Sci* 127:923–928. doi:10.1242/jcs.093773
- 3 11. Juhász G, Hill JH, Yan Y, Sass M, Baehrecke EH, Backer JM, Neufeld TP (2008)
4 The class III PI(3)K Vps34 promotes autophagy and endocytosis but not TOR signaling
5 in *Drosophila*. *J Cell Biol* 181:655–666. doi:10.1083/jcb.200712051
- 6 12. Backer JM (2008) The regulation and function of class III PI3K: novel roles for
7 Vps34. *Biochem J* 410 :1-17. doi:10.1042/BJ20071427.
- 8 13. Yoshioka K, Yoshida K, Cui H, Wakayama T, Takuwa N, Okamoto Y, Du W, Qi
9 X, Asanuma K, Sugihara K, Aki S, Miyazawa H, Biswas K, Nagakura C, Ueno M, Iseki
10 S, Schwartz RJ, Okamoto H, Sasaki T, Matsui O, Asano M, Adams RH, Takakura N,
11 Takuwa Y (2012) Endothelial PI3K-C2 α , a class II PI3K, has an essential role in
12 angiogenesis and vascular barrier function. *Nat Med* 18:1560–1569.
13 doi:10.1038/nm.2928
- 14 14. Posor Y, Eichhorn-Gruenig M, Puchkov D, Schöneberg J, Ullrich A, Lampe A,
15 Müller R, Zarbakhsh S, Gulluni F, Hirsch E, Krauss M, Schultz C, Schmoranzler J, Noé F,
16 Haucke V (2013) Spatiotemporal control of endocytosis by phosphatidylinositol-3,4-
17 bisphosphate. *Nature* 499:233–237. doi:10.1038/nature12360
- 18 15. Biswas K, Yoshioka K, Asanuma K, Okamoto Y, Takuwa N, Sasaki T, Takuwa Y
19 (2013) Essential role of class II phosphatidylinositol-3-kinase-C2 α in sphingosine 1-
20 phosphate receptor-1-mediated signaling and migration in endothelial cells. *J Biol Chem*
21 288:2325–2339. doi:10.1074/jbc.M112.409656
- 22 16. Aki S, Yoshioka K, Okamoto Y, Takuwa N, Takuwa Y (2015)
23 Phosphatidylinositol 3-kinase class II α -isoform PI3K-C2 α is required for transforming

1 growth factor β -induced smad signaling in endothelial cells. *J Biol Chem* 290:6086–6105.
2 doi:10.1074/jbc.M114.601484

3 17. Marat AL, Wallroth A, Lo WT, Müller R, Norata GD, Falasca M, Schultz C,
4 Haucke V (2017) mTORC1 activity repression by late endosomal phosphatidylinositol
5 3,4-bisphosphate. *Science* 356:968–972. doi:10.1126/science.aaf8310

6 18. Rozycka M, Lu YJ, Brown RA, Lau MR, Shipley JM, Fry MJ (1998) cDNA
7 cloning of a third human C2-domain-containing class II phosphoinositide 3-kinase, PI3k-
8 C2 γ , and chromosomal assignment of this gene (PIK3C2G) to 12p12. *Genomics* 54:569–
9 574. doi:10.1006/geno.1998.5621

10 19. Falasca M, Maffucci T (2012) Regulation and cellular functions of class II
11 phosphoinositide 3-kinases. *Biochem J* 443:587–601. doi:10.1042/BJ20120008

12 20. Kitatani K, Usui T, Sriaman SK, Toyoshima M, Ishibashi M, Shigeta S, Nagase S,
13 Sakamoto M, Ogiso H, Okazaki T, Hannun YA, Torchilin VP, Yaegashi N (2016)
14 Ceramide limits phosphatidylinositol-3-kinase C2 β -controlled cell motility in ovarian
15 cancer: potential of ceramide as a metastasis-suppressor lipid. *Oncogene* 35:2801-2812.
16 doi:10.1038/onc.2015.330.

17 21. Domin J, Gaidarov I, Smith ME, Keen JH, Waterfield MD (2000) The class II
18 phosphoinositide 3-kinase PI3K-C2 α is concentrated in the trans-Golgi network and
19 present in clathrin-coated vesicles. *J Biol Chem* 275(16):11943–11950.
20 doi:10.1074/jbc.275.16.11943

21 22. Gaidarov I, Smith ME, Domin J, Keen JH (2001) The class II phosphoinositide 3-
22 kinase C2 α is activated by clathrin and regulates clathrin-mediated membrane trafficking.
23 *Mol Cell* 7:443–449. doi:10.1016/S1097-2765(01)00191-5

- 1 23. Zhao Y, Gaidarov I, Keen JH (2007) Phosphoinositide 3-kinase C2 α links clathrin
2 to microtubule-dependent movement. *J Biol Chem* 282:1249–1256.
3 doi:10.1074/jbc.M606998200
- 4 24. Merrifield CJ, Qualmann B, Kessels MM, Almers W (2004) Neural Wiskott
5 Aldrich Syndrome Protein (N-WASP) and the Arp 2/3 complex are recruited to sites of
6 clathrin-mediated endocytosis in cultured fibroblasts. *Eur J Cell Biol* 83:13–18.
7 doi:10.1078/0171-9335-00356
- 8 25. Benesch S, Polo S, Lai FP, Anderson KI, Stradal TE, Wehland J, Rotter K (2005)
9 N-WASP deficiency impairs EGF internalization and actin assembly at clathrin-coated
10 pits. *J Cell Sci* 118:3103–3115. doi:10.1242/jcs.02444
- 11 26. Galovic M, Xu D, Areces LB, van der Kammen, Innocenti M (2011) Interplay
12 between N-WASP and CK2 optimizes clathrin-mediated endocytosis of EGFR. *J Cell Sci*
13 124:2001–2012. doi:10.1242/jcs.081182
- 14 27. Hussain NK, Yamabhai M, Ramjaun AR, Guy AM, Baranes D, O’Bran JP, Der
15 CJ, Kay BK, McPherson PS (1999) Splice variants of intersectin are components of the
16 endocytic machinery in neurons and nonneuronal cells.
17 *J Biol Chem* 274:15671–15677. doi:10.1074/jbc.274.22.15671
- 18 28. Almeida-Souza L, Frank RAW, García-Nafría J, Colussi A, Gunawardana N,
19 Johson CM, Yu M, Howard G, Andrews B, Vallis Y, McMahon HT (2018) A flat BAR
20 protein promotes actin polymerization at the base of clathrin-coated pits. *Cell* 174: 325–
21 337. doi:10.1016/j.cell.2018.05.020
- 22 29. Das M, Scappini E, Martin NP, Wong KA, Dunn S, Chen YJ, Miller SL, Domin J,
23 O’Bran JP (2007) Regulation of neuron survival through an intersectin-phosphoinositide

- 1 3'-kinase C2 β -AKT pathway. *Mol Cell Biol* 27:7906–17. doi:10.1128/MCB.01369-07
- 2 30. Leverrier Y, Okkenhaug K, Sawyer C, Bilancio A, Vanhaesebroeck B, Ridley AJ
3 (2003) Class I phosphoinositide 3-kinase p110 β is required for apoptotic cell and Fc γ
4 receptor-mediated phagocytosis by macrophages. *J Biol Chem* 278:38437–38442.
5 doi:10.1074/jbc.M306649200
- 6 31. Tamura N, Hazeki K, Okazaki N, Kametani Y, Murakami H, Takaba Y, Ishikawa
7 Y, Nigorikawa K, Hazeki O (2009) Specific role of phosphoinositide 3-kinase p110 α in
8 the regulation of phagocytosis and pinocytosis in macrophages. *Biochem J* 423:99–108.
9 doi:10.1042/BJ20090687
- 10 32. Lim JP, Gleeson PA (2011) Macropinocytosis: An endocytic pathway for
11 internalising large gulps. *Immunol Cell Biol* 89:836–843. doi:10.1038/icb.2011.20
- 12 33. Araki N, Johnson MT, Swanson JA (2012) A role for phosphoinositide 3-kinase
13 in the completion of macropinocytosis and phagocytosis by macrophages. *J Cell Biol*
14 135:1249–1260. doi:10.1083/jcb.135.5.1249
- 15 34. Hoeller O, Bolourani P, Clark J, Stephen LR, Hawkins PT, Weiner OD, Weeks G,
16 Kay RR (2013) Two distinct functions for PI3-kinases in macropinocytosis. *J Cell Sci*
17 126:4296–4307. doi:10.1242/jcs.134015
- 18 35. Nemazany I, Montagnac G, Russell RC, Morzygold L, Burnol AF, Guan KL,
19 Pende M, Panasyuk G (2015) Class III PI3K regulates organismal glucose homeostasis
20 by providing negative feedback on hepatic insulin signalling. *Nat Commun* 6:8283.
21 doi:10.1038/ncomms9283
- 22 36. Law F, Seo JH, Wang Z, Deleon JL, Bolis Y, Brown A, Zong WX, Du G,
23 Rocheleau CE (2017) The VPS34 PI3K negatively regulates RAB-5 during endosome

1 maturation. *J Cell Sci* 130:2007–2017. doi:10.1242/jcs.194746

2 37. Gulluni F, Martini M, De Santis MC, Campa CC, Ghigo A, Margaria JP, Ciruolo
3 E, Franco I, Ala U, Annaratone L, Disalvatore D, Bertalot G, Viale G, Noatynska A,
4 Compagno M, Sigismund S, Montemurro F, Thelen M, Fan F, Meraldi P, Marchio C,
5 Pece S, Sapino A, Chiarle R, Di Fiore PP, Hirsch E (2017) Mitotic spindle assembly and
6 genomic stability in breast cancer require PI3K-C2 α scaffolding function. *Cancer Cell*
7 32: 444-459. doi:10.1016/j.ccell.2017.09.002

8 38. Domin J, Pages F, Volinia S, Rittenhouse SE, Zvelebil MJ, Stein RC, Waterfield
9 MD (1997) Cloning of a human phosphoinositide 3-kinase with a C2 domain that
10 displays reduced sensitivity to the inhibitor wortmannin. *Biochem J* 15: 326 (Pt 1):139-
11 147. doi: 10.1042/bj3260139

12 39. Stein RC, Waterfield MD (2000) PI3-kinase inhibition: a target for drug
13 development? *Mol Med Today* 6:347-357. doi: 10.1016/S1357-4310(00)01770-6

14 40. Katso RM, Pardo OE, Palamidessi A, Franz CM, Marinov M, De Laurentiis A,
15 Downward J, Scita G, Ridley AJ, Waterfield MD, Arcaro A (2006). Phosphoinositide
16 3-Kinase C2 beta regulates cytoskeletal organization and cell migration via Rac-
17 dependent mechanisms. *Mol Biol Cell*.17: 3729-44. doi: 10.1091/mbc.e05-11-1083

18 41. Wang H, Lo WT, Vujičić Žagar A, Gulluni F, Lehmann M, Scapozza L, Haucke
19 V, Vadas O (2018) Autoregulation of class II alpha PI3K activity by its lipid-binding PX-
20 C2 domain module. *Mol Cell* 71:343–351. doi:10.1016/j.molcel.2018.06.042

21 42. Merrifield CJ, Feldman ME, Wan L, Almers W (2002) Imaging actin and
22 dynamin recruitment during invagination of single clathrin-coated pits. *Nat Cell Biol*
23 4:691–698. doi: 10.1038/ncb837

1 43. Yarar D, Waterman-Storer CM, Schmid SL (2005) A dynamic actin cytoskeleton
2 functions at multiple stages of clathrin-mediated endocytosis. *Mol Biol Cell* 16:964–975.
3 doi:10.1091/mbc.e04-09-0774

4 44. Kaksonen M, Toret CP, Drubin DG (2006) Harnessing actin dynamics for
5 clathrin-mediated endocytosis. *Nat Rev Mol Cell Biol* 7:404–414. doi:10.1038/nrm1940

6

7

1 **Figure Legends**

2 **Fig. 1 Class II PI3K-C2 α and PI3K-C2 β are necessary for fluid-phase pinocytosis in**

3 **HUVECs. (a , b)** Time-dependent uptake of FITC-dextran. Cells were incubated with

4 FITC-dextran (0.2 mg/ml) in growth medium at 37°C for indicated time periods,

5 followed by fixation with 4% PFA. Nuclei were stained with DAPI (blue). Scale bar, 20

6 μ m. **(a)** Representative images showing internalized FITC-dextran (green dots) at each

7 time point. **(b)** Quantified data. n = 50-60 cells were analyzed in each group. The green

8 dots were quantified as described as “Materials and Methods” (*right*). **(c)** siRNA-

9 mediated knockdown of PI3K isoforms. Representative Western blots showing siRNA-

10 mediated knockdown of PI3K protein expression after 48 hr post-transfection (*left*). Cells

11 were transfected with either PI3K-C2 α -, PI3K-C2 β -, p110 α - or Vps34-specific siRNA or

12 scrambled siRNA. GAPDH was used as loading control. Quantified data of protein

13 expression levels (*right*). **(d , e)** Effects of knockdown of different PI3K isoforms on

14 FITC-dextran uptake. Cells were incubated with FITC dextran for 45 min. **(d)**

15 representative images. **(e)** quantified data. **(f)** Effects of different PI3K inhibitors on

16 FITC-dextran uptake. Cells were pretreated with 0.1 μ M of GDC 0941, 1mM of 3-MA, or

17 30 nM and 1 μ M of wortmannin (WMN) for 30 min and then subjected to FITC-dextran

18 uptake assay. Scale bar, 20 μ m. Asterisks indicate statistical significance between the

19 indicated groups; * p < 0.05, **p < 0.01, ***p < 0.001. data are means \pm SEM in Fig (c)

20 and median and interquartile range in Fig (b)(e)(f).

21

22 **Fig. 2 Pinocytosis is partially dependent on clathrin and dynamin in HUVECs. (a)**

23 Effects of the clathrin inhibitor Pitstop-2 on FITC-dextran uptake. Cells were pretreated

1 with either Pitstop-2 (20 μ M) or vehicle for 30 min and then subjected to FITC-dextran
2 uptake assay. Upper, representative images. Scale bar, 20 μ m. Lower, quantified data. **(b)**
3 Effects of clathrin heavy chain (CHC) knockdown on FITC-dextran uptake. Cells were
4 transfected with either scrambled or CHC-siRNA. Left upper, representative images; left
5 lower, quantified data of FITC-dextran uptake. Right upper, representative blots of CHC
6 protein; right lower, quantified data of protein expression levels. **(c)** Effects of the
7 expression of mRFP-tagged dominant negative dynamin-2 (K44A) mutant (dn-Dyn2) on
8 FITC-dextran uptake. Cells were transfected with either mRFP-tagged wild type
9 dynamin2 (wt-Dyn2) or dn-Dyn2, and 24 hr later subjected to FITC-dextran uptake.
10 Upper, representative images of cells. Nuclei were stained with DAPI (blue). Lower,
11 quantified data of FITC-dextran uptake. n = 50-60 cells were analyzed in each group.
12 Data are median and interquartile range in (a), (b, *lower left*) and (c), and means \pm SEM
13 in (b, *lower right*). Asterisks indicate statistical significance between the indicated
14 groups; * p < 0.05, **p < 0.01, ***p < 0.001.

15

16 **Fig. 3 Partially overlapping subcellular localization of PI3K-C2 α and PI3K-C2 β in**
17 **HUVECs.** **(a)** Cells were cotransfected with the expression vectors of GFP-C2 α and
18 mCherry-C2 β , and imaged by confocal microscopy coupled with Super-Resolution
19 Radial Fluctuation (SRRF)-Stream mode. Nuclei were stained with DAPI (blue). Note
20 that cytoplasmic fine puncta of GFP-C2 α (*left*) and coarse and fine puncta of mCherry-
21 C2 β (*middle*) surrounding the podosomes and on plasma membrane (*white arrowheads*)
22 and perinuclear coarse puncta of mCherry-C2 β (*yellow arrows*). White arrowheads in
23 SRRF view of the merged image indicate the colocalization of GFP-C2 α and mCherry-

1 C2 β . **(b)** Representative confocal microscopic images of GFP-C2 α or mCherry-C2 β and
2 F-actin. Cells transfected with the expression vectors of GFP-C2 α and mCherry-C2 β
3 were stained with iFluor488-conjugated phalloidin (green) or AlexaFlour594-conjugated
4 phalloidin (red). Nuclei were stained with DAPI. White arrowheads indicate the
5 colocalization of F-actin and GFP-C2 α or mCherry-C2 β . Blue arrowheads indicate the
6 colocalization of F-actin and mCherry-C2 β in the membrane ruffle. **(c and d)**
7 Colocalization of GFP-C2 α **(c)** or mCherry-C2 β **(d)** with organelle markers. Cells
8 expressing either GFP-C2 α or mCherry-C2 β were stained with antibodies against CHC
9 (CCS, clathrin-coated structures), EEA1 (EE, early endosomes), Rab7 (LE, late
10 endosomes), LAMP1 (LY, lysosomes) and LC3B (AP, autophagosomes). Nuclei were
11 stained with DAPI (blue). White arrowheads in SRRF views indicate the colocalization
12 of GFP-C2 α or mCherry-C2 β with each organelle markers.

13

14 **Fig. 4 Immunofluorescent staining of endogenous PI3K-C2 β in HUVECs.** Cells were
15 double-immunostained with anti-PI3K-C2 β (green) and AlexaFlour594-conjugated
16 phalloidin (red), anti-CHC (red), anti-EEA1 (red) or anti-LC3B (red), and imaged by
17 confocal microscopy coupled with Super-Resolution Radial Fluctuation (SRRF)-Stream
18 mode. Nuclei were stained with DAPI (blue). Scale bar, 10 μ m. White arrowheads in
19 SRRF views indicate the colocalization of endogenous PI3K-C2 β with each organelle
20 markers.

21

22 **Fig. 5 PI3K-C2 α and PI3K-C2 β are required for clathrin-mediated pinocytosis.**

1 (a) Effects of double knockdown of PI3K-C2 α and -C2 β on FITC-dextran uptake. Cells
2 were transfected with either alone of scrambled-, C2 α - and C2 β -siRNAs (50 nM each) or
3 the combination of C2 α - and C2 β -siRNAs (25 nM each). *Left*, Relative protein
4 expression levels of PI3K-C2 α and -C2 β determined by Western blotting. *Right*, FITC-
5 dextran uptake. (b) No effect of C2 α - and C2 β -knockdown in CHC-depleted HUVECs.
6 The single and double knockdown was performed as described in the "Materials and
7 Methods". After 48 hr later, cells were subjected to FITC-dextran uptake assay as
8 described in (a). (c and d) Super-resolution microscopic images of cells transfected with
9 the expression vectors of mRFP-clathrin light chain (mRFP-CLC, red) and either GFP-
10 C2 α (green in c) or GFP-C2 β (green in d). Nuclei were stained with DAPI (blue). Scale
11 bar, 10 μ m. *Lower*, representative serial images showing the dynamics of PI3K-C2 α (c)
12 and -C2 β (d) association with clathrin. Time zero was set as the peak of clathrin
13 recruitment. See also Supplementary movies 1 and 2. (e) Quantified data of the lower
14 images in (c) and (d). n = 3 and 4 events for C2 α /clathrin and C2 β /clathrin, respectively.
15 (f) The colocalization of GFP-C2 α (*Left*) or -C2 β (*Right*) in clathrin-coated pinocytic
16 vesicles. Super-resolution microscopic images of cells expressing GFP-C2 α (*Left*) or -
17 C2 β (*Right*) and mRFP-CLC that were subjected to AlexaFlour647-dextran uptake.
18 White arrowheads indicate dextran-containing, C2 α - or C2 β -positive pinosomes. (g)
19 Effects of either PI3K-C2 α or -C2 β knockdown on FITC-dextran accumulation in early
20 endosomes. Cells were transfected with scramble, PI3K-C2 α - or -C2 β -siRNAs. Twenty
21 four hours later, the knocked down cells were infected with RFP-Rab5 baculoviral vector,
22 followed by FITC-dextran uptake assay. *Left*, representative images and *right*, quantified
23 data of FITC-dextran⁺, mRFP-Rab5⁺ vesicles and mRFP-Rab5⁺ vesicles. (h) Time-

1 dependent degradation of uptaken FITC-dextran in PI3K-C2 α - and -C2 β -depleted cells.
2 Cells that had been transfected with indicated siRNAs were subjected to FITC-dextran
3 pulse-chase experiments as described in “*Materials and Methods*”. Asterisks indicate
4 statistically significant difference between the indicated groups; * $p < 0.05$, ** $p < 0.01$,
5 *** $p < 0.001$. Nuclei were stained with DAPI (blue). Data are median and interquartile
6 range in (a, *right*), (b), (g) and means \pm SEM in (a, *left*), (e) and (h).

7
8 **Fig. 6 PI3K-C2 β is required for the formation of pinosome-associated actin patches.**

9 (a - c) Super-resolution microscopic images of HUVECs transfected with the expression
10 vectors of mRFP-CLC (*red*) and the F-actin-binding peptide mEmerald-Lifeact (*green*),
11 and either of scrambled (a), PI3K-C2 α - (b) or -C2 β (c)-siRNAs. Cells were then
12 subjected to AlexaFlour647-dextran (0.5 mg/ml) uptake. Nuclei were stained with DAPI
13 (*blue*). The region outlined by the dotted-box is shown at higher magnification (*Upper*,
14 Dextran/F-actin. *Lower*, Clathrin/F-actin) on the right panels. White arrowheads denote
15 clathrin-coated, dextran-containing pinosomes that are associated with actin patches,
16 whereas yellow arrows denote clathrin-non-coated, dextran-containing pinosomes that
17 are associated or not with actin patches. (d) Average number of dextran+-vesicles per cell
18 was quantified from images. (e and f) The co-localization of F-actin and clathrin (e) and
19 dextran and F-actin (f). The colocalization index (Pearson’s correlation coefficient) are
20 shown. Through (d)- (f), Data are represented as median and interquartile range.
21 Asterisks indicate statistical significance between the indicated groups; Asterisks indicate
22 statistical significance between the indicated groups; * $p < 0.05$, ** $p < 0.01$, *** $p <$
23 0.001.

1
2 **Fig. 7 Overexpression of PI3K-C2 β but not PI3K-C2 α enhances dextran uptake in**
3 **the presence of Intersectin-1 overexpression. (a and c)** Super-resolution microscopic
4 images of cells. Cells were transfected with the expression vectors of mCherry or
5 mCherry-C2 β or C2 α (*red*) and GFP or GFP-ITSN1s (*green*). The cells were then
6 subjected to AlexaFlour647-dextran (*purple*). Nuclei were stained with DAPI (*blue*).
7 Merged images of the mCherry and GFP signals in the boxed regions are shown in the
8 *right-lower panels* of the middle (GFP) row, with white arrowheads (yellow-colored
9 dots) indicating the overlap of red and green signals. Yellow asterisks indicate nuclei of
10 vectors-transfected cells. #, nuclei of non-transfected cells. **(b and d)** Upper, average
11 number of dextran⁺ vesicles per cell. Lower, average number of mCherry-C2 β ⁺ **(b)** or
12 mCherry-C2 α ⁺ vesicles **(d)** per cell. Data are represented as median and interquartile
13 range. Asterisks indicate statistical significance between the indicated groups; * $p < 0.05$,
14 ** $p < 0.01$, *** $p < 0.001$.

15
16 **Fig. 8 Intersectin-1 is required for the formation of actin patches and the**
17 **recruitment of PI3K-C2 β to the clathrin-coated structures. (a and b)** Confocal
18 microscopy coupled with Super-Resolution Radial Fluctuation (SRRF)-Stream mode
19 images of cells transfected with scrambled and ITSN1-specific siRNA. Double
20 immunostaining with **(a)** anti-ITSN (*green*) or **(b)** anti-PI3K-C2 β (*green*) antibodies and
21 AlexaFlour594-conjugated phalloidin (*red, left panels*) or anti-CHC antibody (*red, right*
22 *panels*). Nuclei were stained with DAPI (*blue*). The region outlined by the dotted-box is
23 shown at higher magnification. White arrowheads in SRRF view of the merged image

1 indicate the colocalization of endogenous ITSN1 **(a)** or PI3K-C2 β **(b)** with F-actin or
2 clathrin-coated structures.**(c, d)** co-localization index of PI3K-C2 β and F-actin **(c)** or
3 CHC **(d)**. Data are represented as median and interquartile range. Asterisks indicate
4 statistical significance between the indicated groups; * $p < 0.05$, ** $p < 0.01$, *** $p <$
5 0.001.

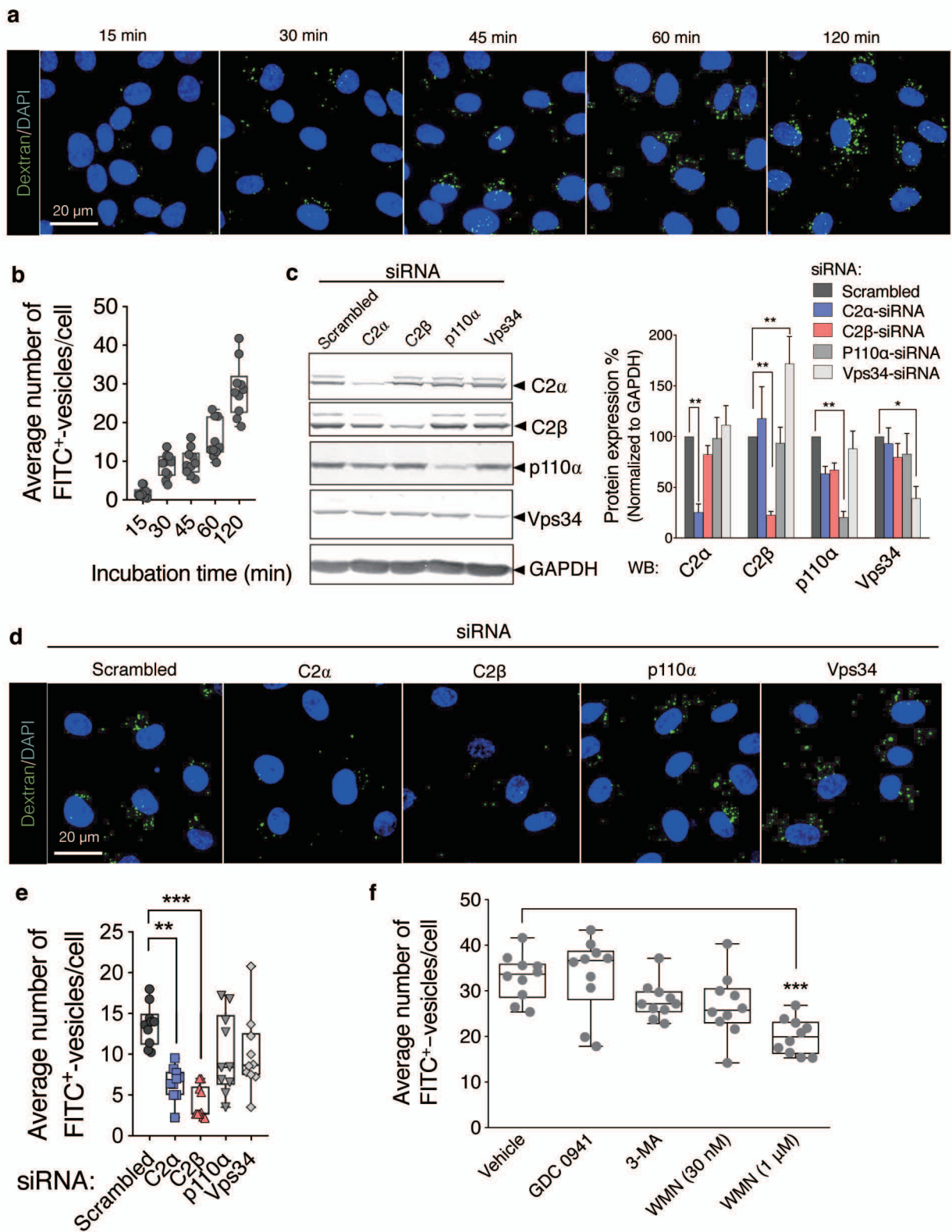


Fig.1 Thuzar *et al.*

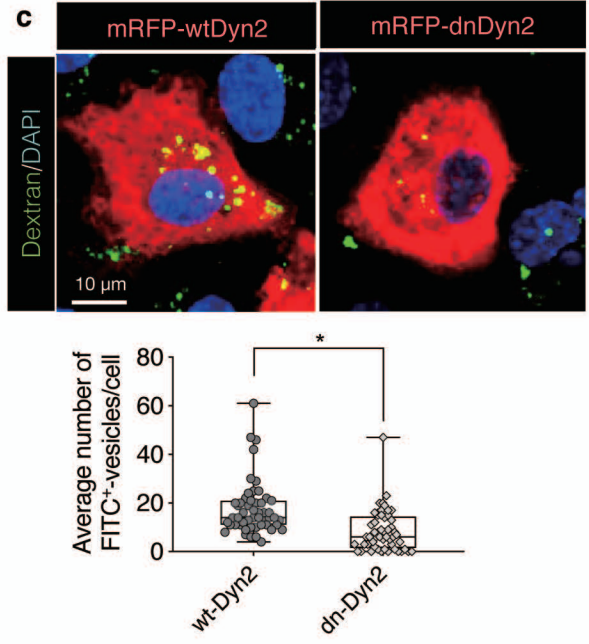
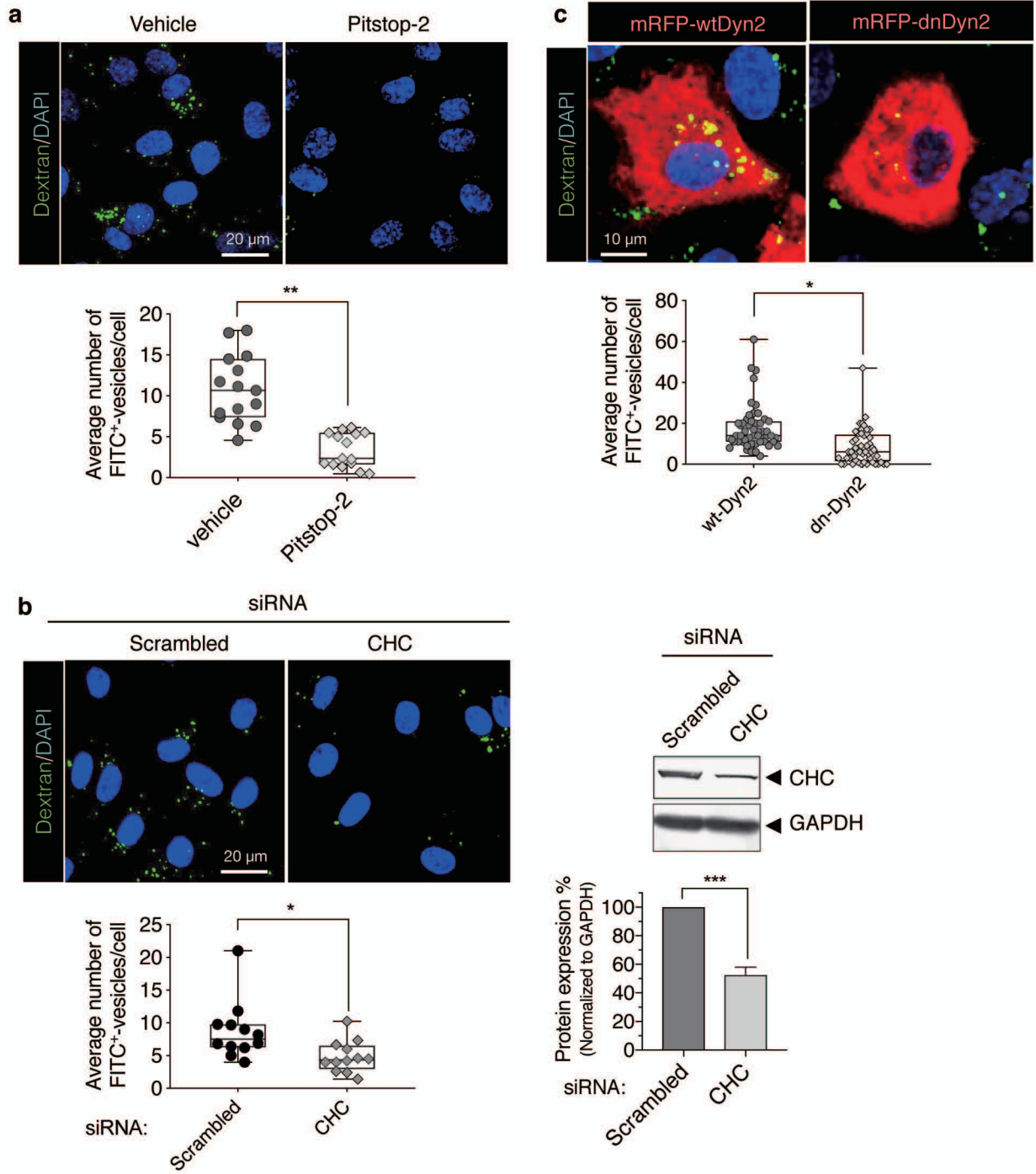


Fig. 2 Thuzar *et al.*

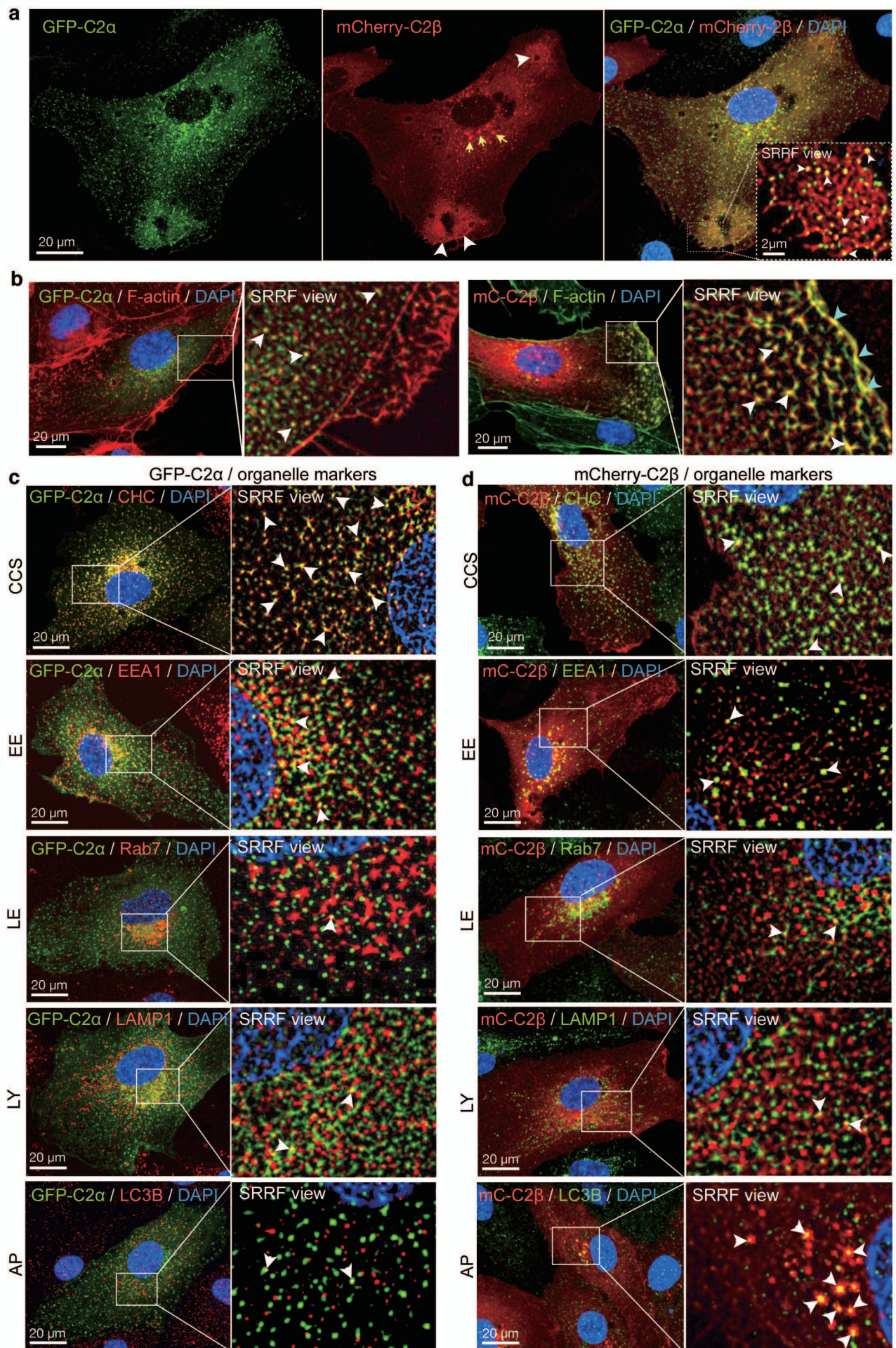


Fig. 3 Thuzar *et al.*

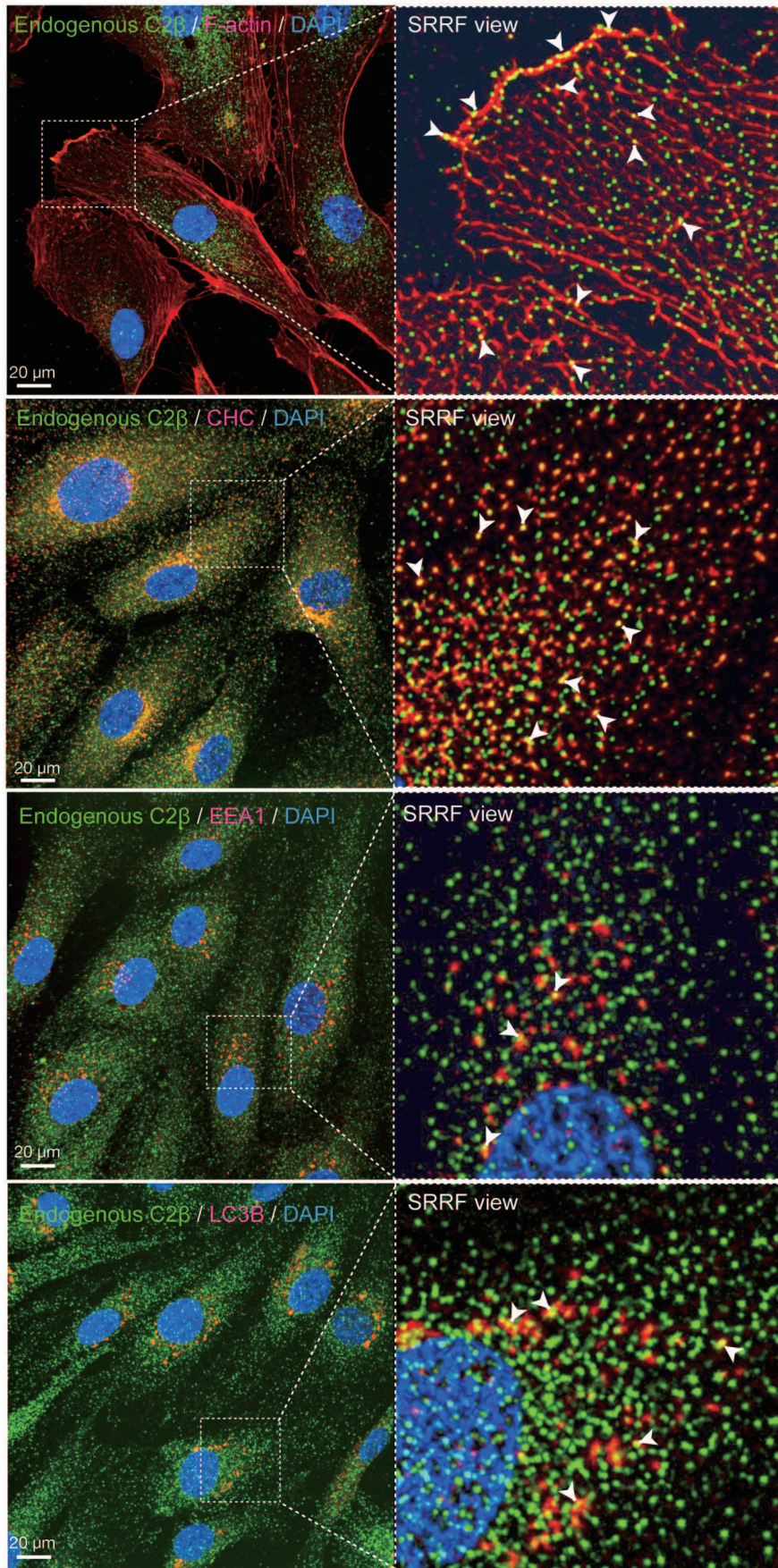


Fig. 4 Thuzar *et al.*

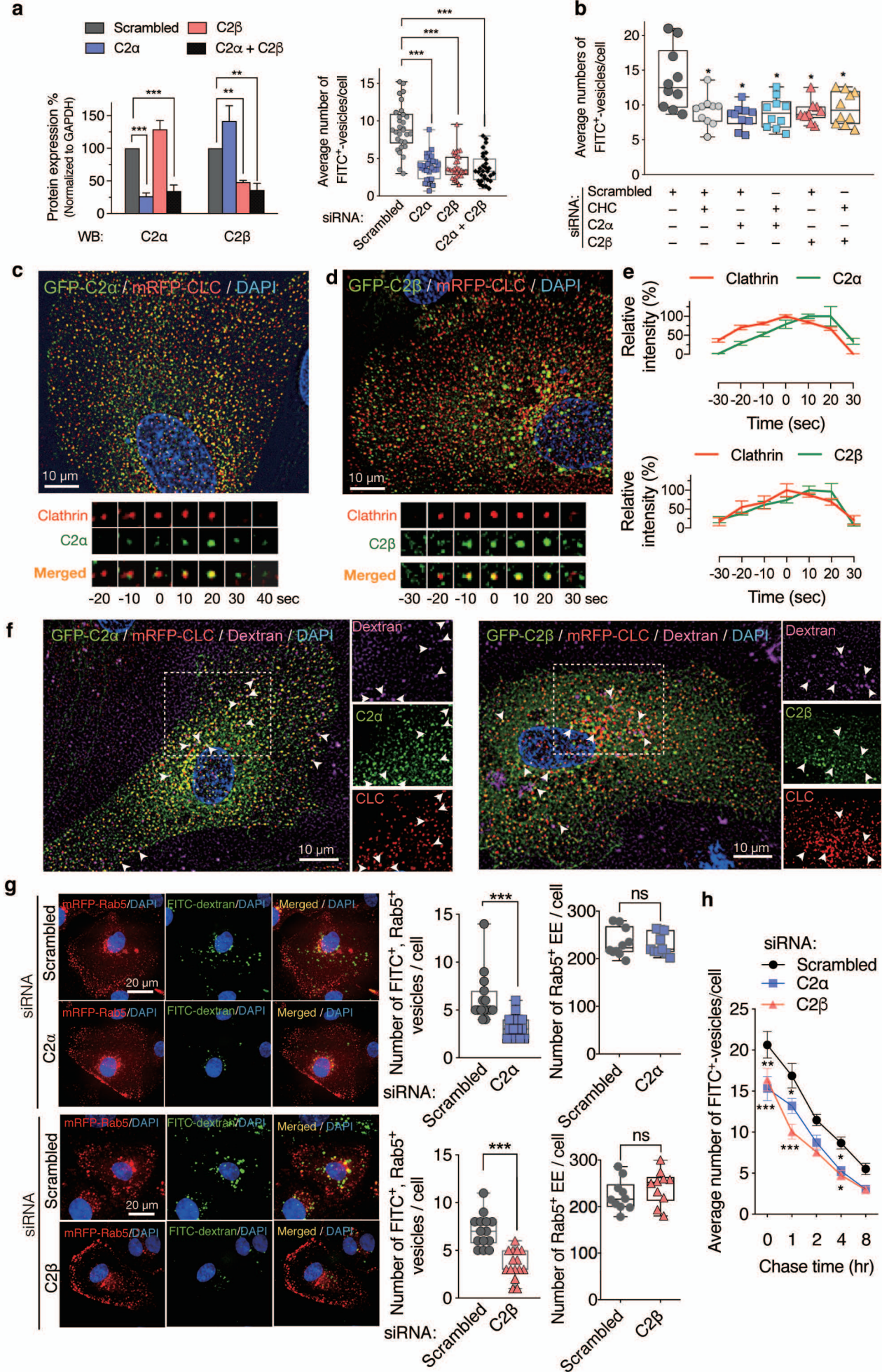


Fig. 5 Thuzar *et al.*

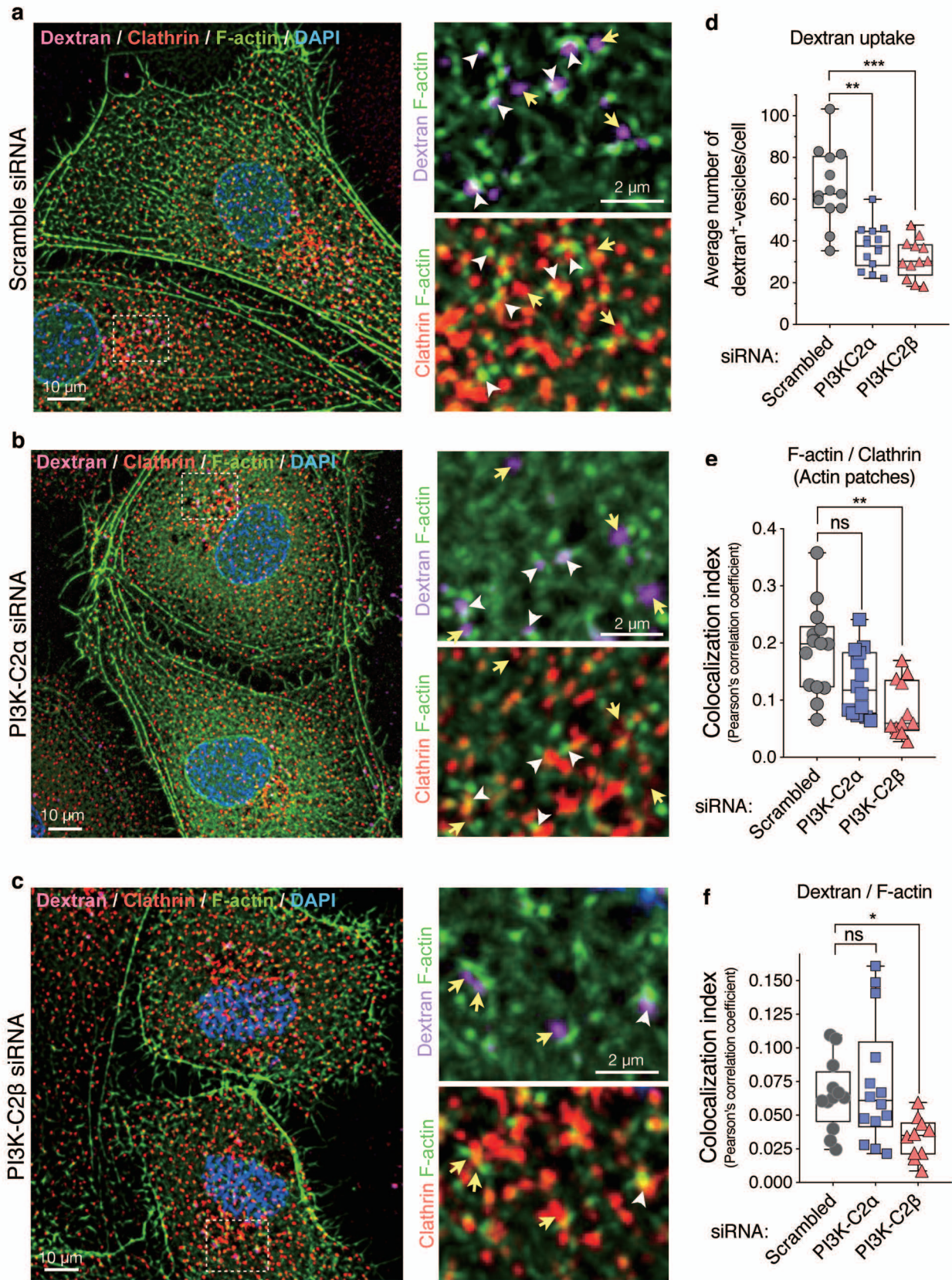


Fig. 6 Thuzar *et al.*

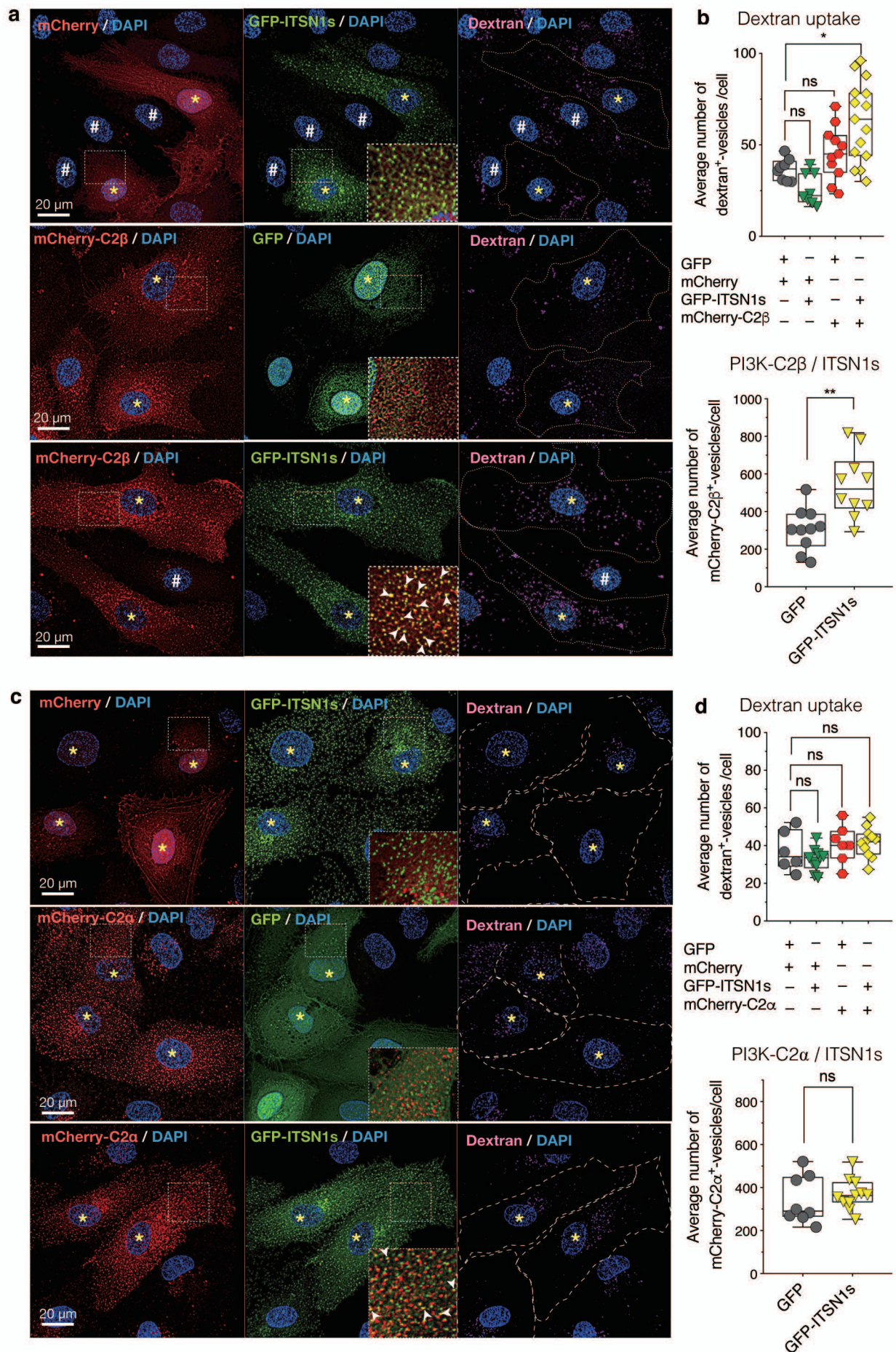


Fig. 7 Thuzar *et al.*

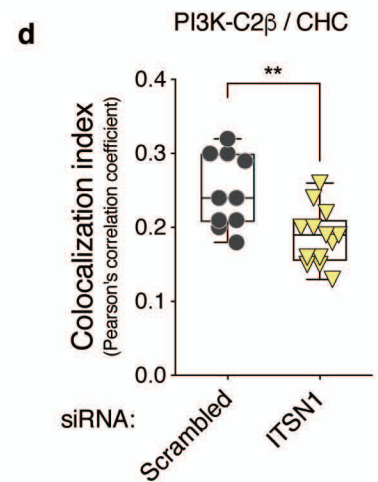
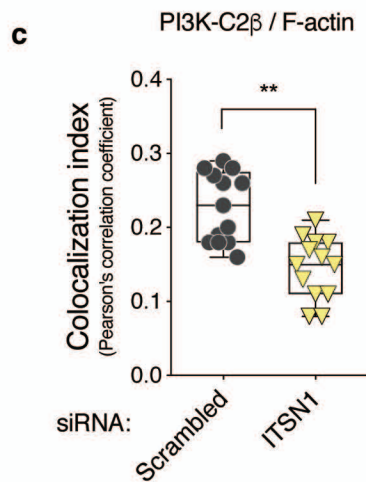
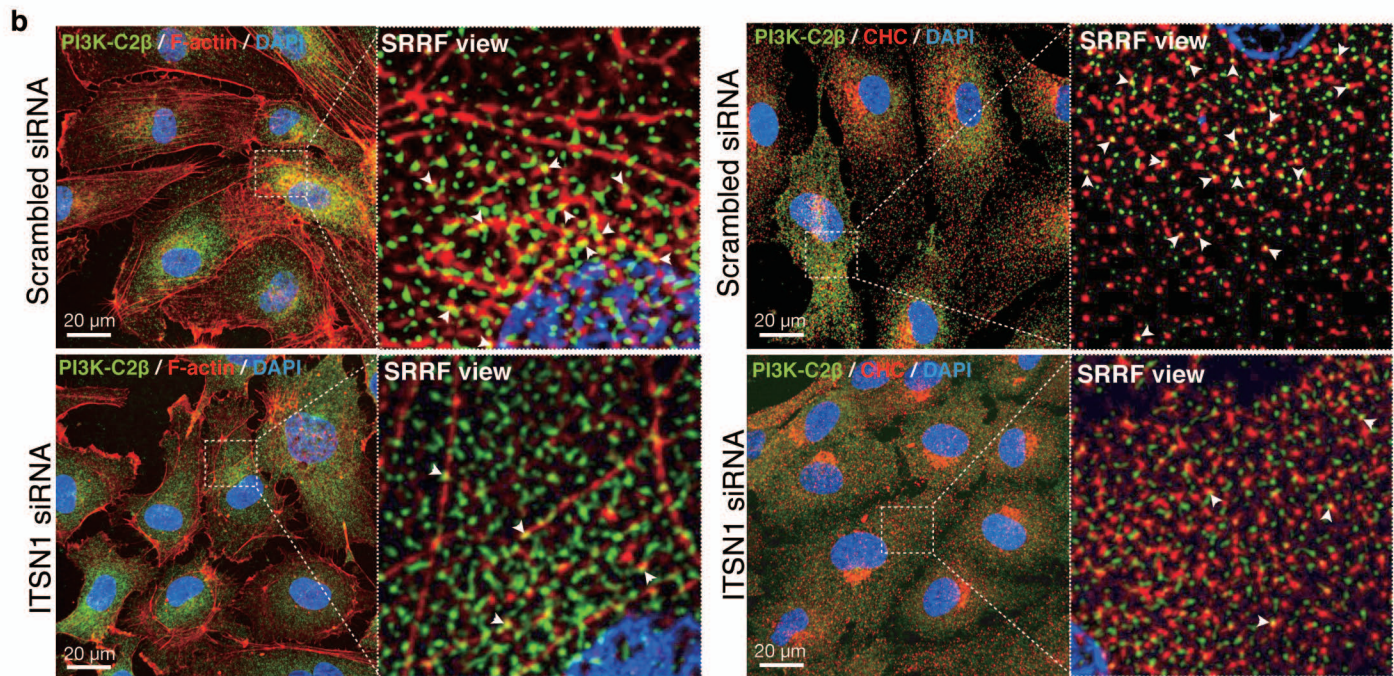
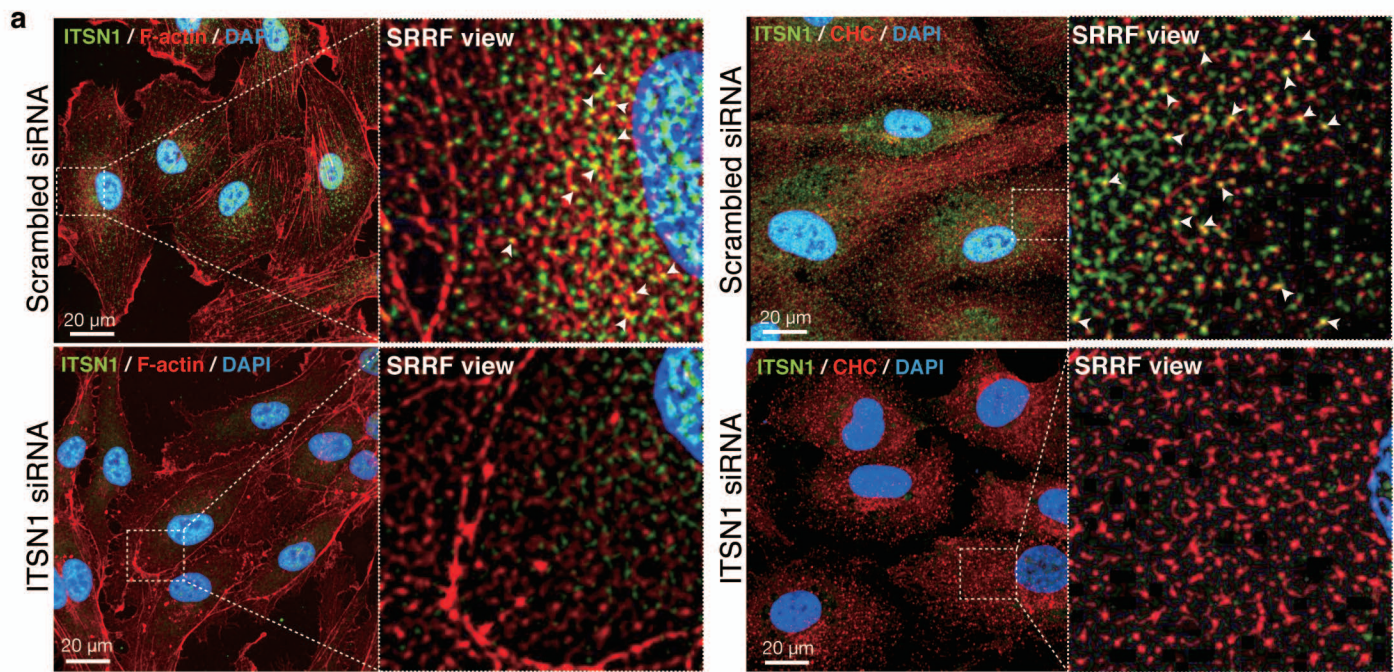


Fig. 8 Thuzar *et al.*